



Escuela
Politécnica
Superior

Retina Vessel Segmentation (Computer Vision)



Master's degree in Artificial Intelligence

Computer Vision

Author:

Cristian Andrés Córdoba Silvestre

Teacher:

Antonio Jorge Pertusa Ibáñez

January 2026

Retina Vessel Segmentation (Computer Vision)

Computer Vision

Author

Cristian Andrés Córdoba Silvestre

Teacher

Antonio Jorge Pertusa Ibáñez



Master's degree in Artificial Intelligence



**Escuela
Politécnica
Superior**



**Universitat d'Alacant
Universidad de Alicante**

ALACANT, January 2026

Abstract

This project addresses the **automatic segmentation of retinal blood vessels** from color fundus images using **classical, fully unsupervised computer-vision techniques**. The work first introduces a robust **retinal field-of-view (FOV) mask extraction** stage to restrict processing to anatomically valid pixels and to mitigate common acquisition artifacts such as **vignetting, illumination gradients, and border truncation**. On top of this preprocessing, five genuinely different vessel-segmentation pipelines are implemented and compared: (A) **green channel + CLAHE + multi-orientation morphological vessel enhancement + thresholding**, (B) morphology-driven enhancement followed by **k -means clustering**, (C) **Retinex-like illumination correction** and morphological vesselness refined with **graph-cut (GrabCut)**, (D) morphology with explicit **connected-components structural filtering**, and (E) candidate generation plus a stronger **shape-constrained connected-components rejection** stage.

Moreover, a systematic **grid search** is used to tune each pipeline, and performance is quantified with **IoU statistics and runtime per image**. Results show that a carefully tuned morphology-and-threshold baseline (Pipeline A) achieves the best overall accuracy (**mean IoU $\approx 0,55$**) with competitive execution time, while other pipelines reveal clear speed–accuracy trade-offs and failure modes that motivate practical design recommendations.

The future depends on what you do today.

— Mahatma Gandhi

Table of Contents

List of figures	11
List of tables	11
1 Detection of the Retina's Region	15
1.1 FOV/retina mask extraction	15
2 Implementations of the different Pipelines	17
2.1 Pipeline A: Green channel → CLAHE → morphology → threshold	17
2.2 Pipeline B: Morphology → k-means → cleanup	20
2.3 Pipeline C: Illumination correction → vessel enhancement → Graph Cut . . .	23
2.4 Pipeline D: Multi-orientation morphology + connected	25
2.5 Pipeline E: Use of CC mainly as structural filtering, not as a primary segmenter	28
3 Comparison and Conclusion	33

List of figures

1.1	Retina Mask Extraction	16
2.1	Vessel Segmentation for Image 12.png: IoU=0.614325	18
2.2	Vessel Segmentation for Image 13.png: IoU=0.602988	18
2.3	All Steps for Image 12.png: IoU = 0.619938	19
2.4	Best Grid for all Paramater Combinations for Pipeline A	19
2.5	Vessel Segmentation for Image 8.png: IoU=0.554655	21
2.6	Vessel Segmentation for Image 13.png: IoU=0.549874	21
2.7	Best Grid for all Paramater Combinations for Pipeline B	22
2.8	Vessel Segmentation for Image 9.png: IoU=0.558516	23
2.9	Vessel Segmentation for Image 20.png: IoU=0.562874	24
2.10	Best Grid for all Paramater Combinations for Pipeline C	24
2.11	Vessel Segmentation for Image 13.png: IoU=0.455248	26
2.12	Vessel Segmentation for Image 15.png: IoU=0.431216	27
2.13	Best Grid for all Paramater Combinations for Pipeline D	27
2.14	Vessel Segmentation for Image 20.png: IoU=0.560231	29
2.15	Vessel Segmentation for Image 13.png: IoU=0.556936	30
2.16	Best Grid for all Paramater Combinations for Pipeline E	30

List of tables

2.1	Pipeline A variant ranking after grid search	20
2.2	Pipeline B variant ranking after grid search	22
2.3	Pipeline C variant ranking after grid search	25
2.4	Pipeline D variant ranking after grid search	28
2.5	Pipeline E variant ranking after grid search	31

3.1 Best variant per pipeline after grid search (IoU statistics, runtime, and foreground fraction when available)	33
---	----

1. Detection of the Retina's Region

1.1 FOV/retina mask extraction

URL¹ of the GitHub repository.

This technique isolates the retinal field of view as a clean binary region so that subsequent vessel segmentation is restricted to anatomically valid pixels and is not contaminated by the dark peripheral background. In our implementation (`compute_fov_mask`), this is achieved by converting the input to a single informative channel (the green channel when available, otherwise grayscale), applying a light denoising blur (median or Gaussian with an odd kernel size) to suppress small-scale noise, and performing an illumination-normalization («flat-field») correction by dividing the blurred image by a heavily smoothed estimate of the background illumination and re-normalizing to [0, 255]. This stabilizes global thresholding under vignetting and resembles the inhomogeneity-correction motivation emphasized in Retinex-based retinal pipelines (e.g., the role of illumination correction discussed in the Retinex framework of Zhao et al., 2015). On the corrected image, an Otsu global threshold is computed and, to remain robust to contrast polarity, both the raw threshold and its inversion are considered as competing foreground hypotheses, each cleaned by morphological closing followed by opening with elliptic structuring elements (kernel sizes are either user-specified or automatically scaled to image geometry). Afterward, only the largest connected component is retained to represent the contiguous retina.

A simple, explicitly defined heuristic scoring function (favoring plausible area ratio, centrality, low border contact, and compactness/circularity) selects between the normal and inverted candidates to prevent pathological selections on atypical images. Finally, the mask is refined by hole filling via border-seeded flood fill (to remove internal gaps), optional convex-hull regularization (to enforce a disk-like FOV consistent with morphological shape priors), and an additional, targeted ellipse-fitting mechanism designed to correct the «straight bite/chord cut» failure mode that convexification cannot fix. An automatic test compares the filled region's area to its minimum-enclosing-circle area, and if the fill ratio is suspiciously low the algorithm fits an ellipse from edge points in a narrow ring around the boundary (Canny on the corrected image with thresholds derived from the median intensity inside the FOV), with a conservative scale factor to recover small border losses and a fallback to contour-based `fitEllipse`.

¹URL of the GitHub Repository containing the code of the project": <https://github.com/cacs2-ua/tva-final-practice.git>

The output is a strict 0/255 uint8 mask that is both reproducible and computationally inexpensive, and it operationalizes well-established morphological cleaning principles frequently used in retinal preprocessing while adding explicit safeguards for illumination gradients and common FOV truncation artifacts.

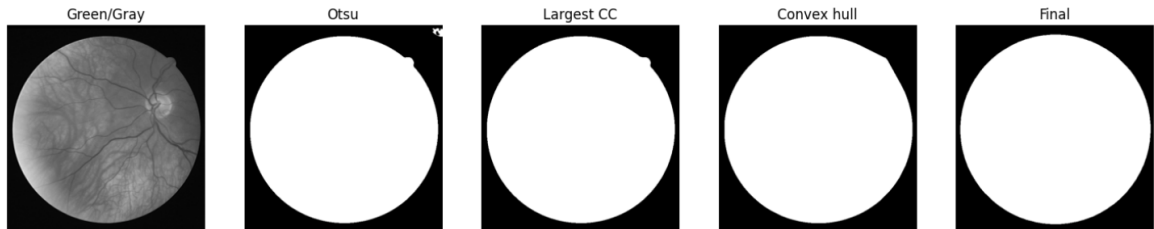


Figure 1.1: Retina Mask Extraction

2. Implementations of the different Pipelines

2.1 Pipeline A: Green channel → CLAHE → morphology → threshold

This pipeline implements a baseline that converts a color fundus image into a binary vessel mask by chaining local-contrast normalization, morphology-based vessel enhancement, global/local thresholding, and lightweight post-processing, while strictly restricting all operations to anatomically plausible pixels via the previously computed FOV mask (Step 1) so that the dark peripheral background does not bias either enhancement or threshold selection.

Concretely, given an input image, the implementation first extracts the green channel (empirically the most vessel-informative channel in standard color fundus photography) and applies CLAHE to improve local vessel–background separability. To prevent artificial contrast amplification at the FOV boundary, pixels outside the mask are filled with a robust inside-FOV statistic (the median intensity) before CLAHE, and are then zeroed again after equalization so subsequent processing is purely intra-retinal.

Vessel enhancement is then performed using mathematical morphology: a black-hat transform (or, equivalently, a top-hat on the inverted intensity) is applied with multiple oriented line-shaped structuring elements spanning several lengths and evenly sampled angles, and the maximum response across orientations and scales is taken as a «vesselness» map. Optionally, additional isotropic disk black-hat responses are fused by a max operator to better capture thicker vessels that are not well matched by thin line kernels. This design directly encodes the anatomical prior that vessels are locally dark, elongated, and appear at multiple orientations and widths, aligning with morphology-centric retinal vessel pipelines and with the broader observation that CLAHE is an effective local-contrast step in retinal analysis.

The vesselness map is lightly smoothed (small Gaussian blur) and binarized either by Otsu thresholding computed only from FOV pixels (to avoid background-driven bias) or by adaptive Gaussian thresholding. In the Otsu branch, the code further stabilizes per-image behavior by automatically adjusting the effective threshold via an offset sweep when the initial foreground fraction becomes implausibly small/large, and, if needed, falling back to a percentile-based unsupervised threshold targeting a realistic vessel occupancy, thereby mitigating the common «single-image collapse» failure mode.

Finally, the binary mask is cleaned by morphological opening/closing to suppress speckle noise and reconnect small gaps, and by connected-components filtering that removes regions below a minimum area, yielding a computationally inexpensive 0/255 uint8 vessel segmentation suitable as a robust baseline.

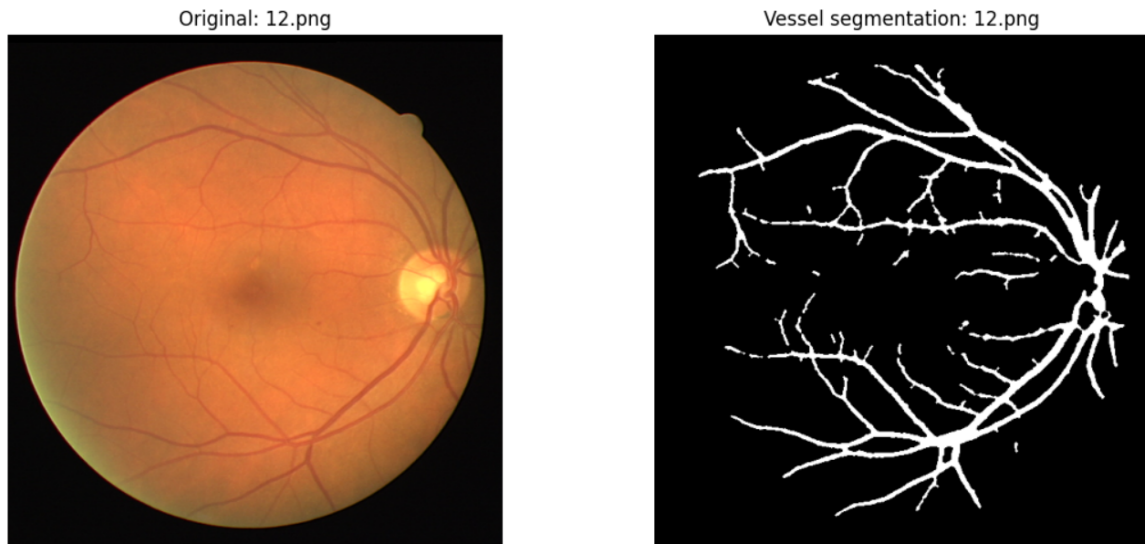


Figure 2.1: Vessel Segmentation for Image 12.png: IoU=0.614325

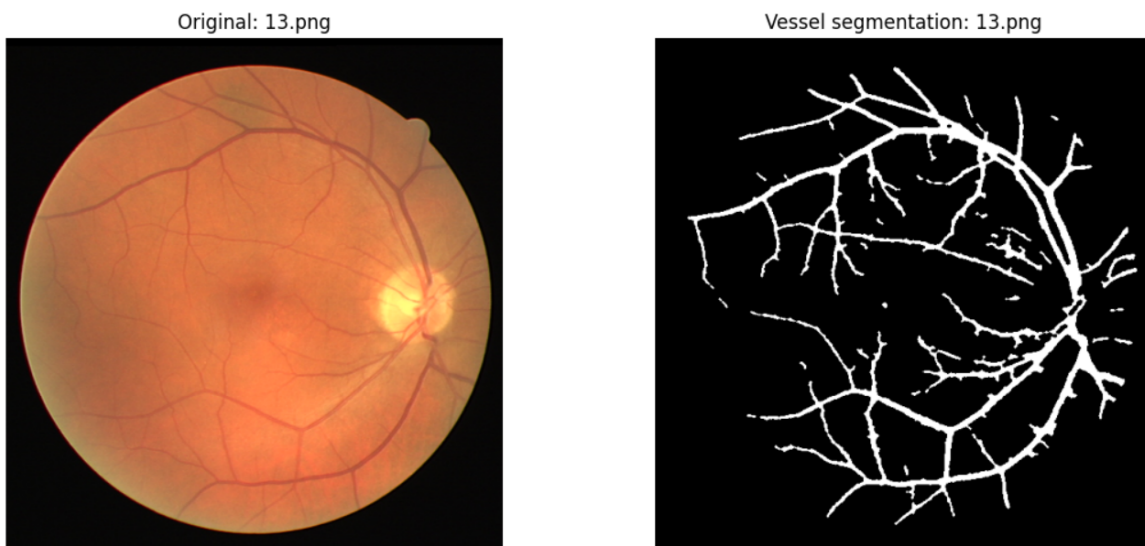


Figure 2.2: Vessel Segmentation for Image 13.png: IoU=0.602988

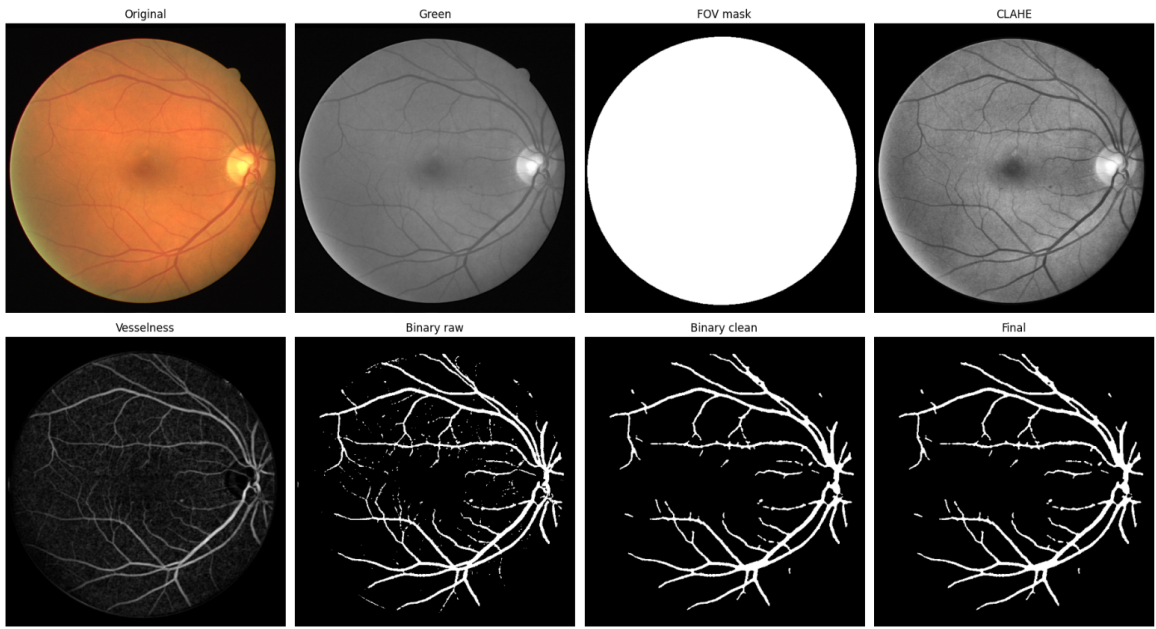


Figure 2.3: All Steps for Image 12.png: IoU = 0.619938

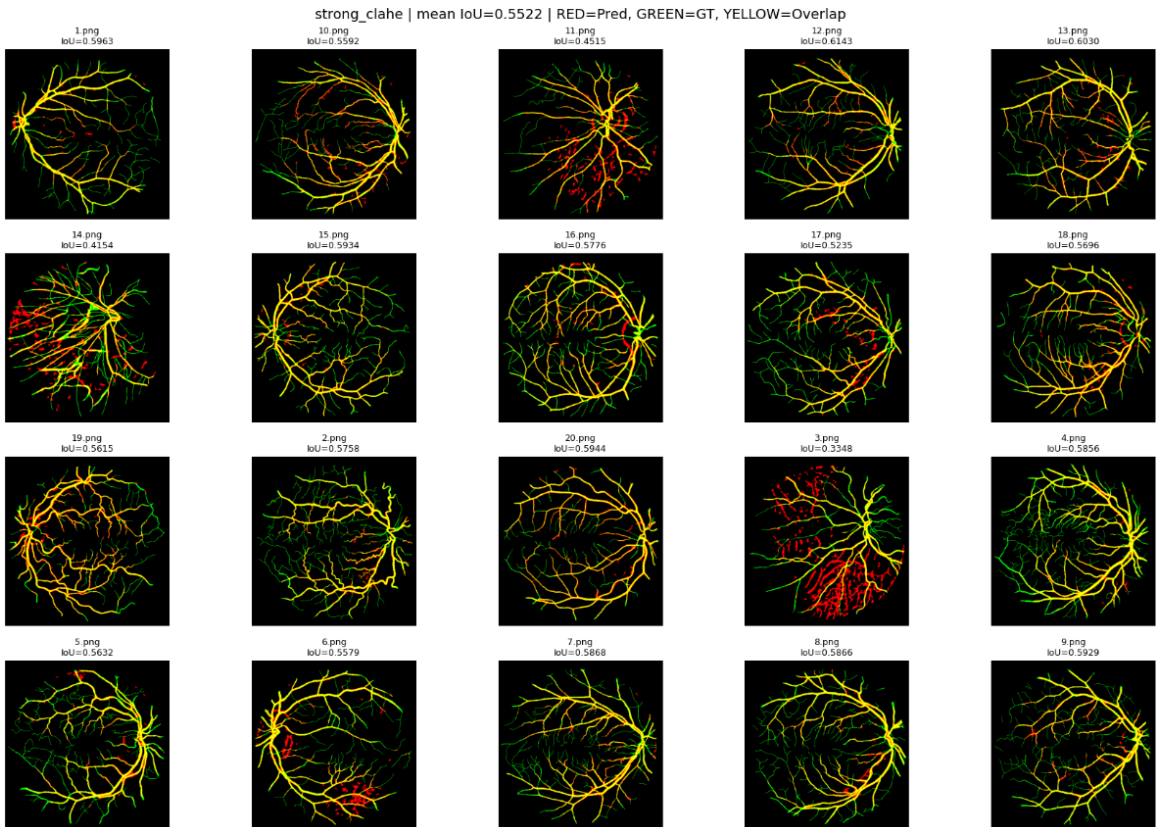


Figure 2.4: Best Grid for all Parameter Combinations for Pipeline A

Rank	Variant	Mean IoU	Median IoU	Std. IoU	Min IoU	Max IoU	Time (s/img)
01	strong_clahe	0.552167	0.576725	0.069193	0.334794	0.614325	0.692420
02	fov_tight	0.550735	0.565960	0.061267	0.371730	0.620463	0.665983
03	baseline	0.550663	0.568422	0.061033	0.371598	0.619938	0.726917
04	tophat_invert	0.549480	0.567525	0.061501	0.372280	0.620469	0.680961
05	thick_bias	0.538735	0.564334	0.063446	0.343411	0.607285	0.691477
06	balanced_plus	0.531191	0.561013	0.065809	0.336492	0.597293	0.670545
07	sensitive_thin	0.520336	0.545978	0.077858	0.328285	0.595987	0.717001
08	adaptive_thr	0.471890	0.489644	0.071506	0.262879	0.565206	0.754745
09	precision_fp	0.381377	0.383932	0.054243	0.260503	0.465405	0.653867

Notes. Performance summary for Pipeline A variants in the retinal vessel segmentation task, sorted by mean IoU (higher is better). Times are reported as seconds per image.

Table 2.1: Pipeline A variant ranking after grid search

All of the different parameters used in each variant can be seen in the `.ipynb` file of the project.

2.2 Pipeline B: Morphology → k-means → cleanup

In this Pipeline, mathematical morphology is used to suppress background variability and emphasize vessel-like structures, and k -means clustering is then applied to separate vessels from non-vessels.

Local contrast is normalized with CLAHE to increase separability of thin vessels under mild illumination non-uniformities.

Vessel boosting is then performed via multi-orientation, line-structuring-element morphology: we compute a directional black-hat response on the CLAHE image (to enhance dark, elongated lines) and, in parallel, a top-hat response on the inverted image (to handle contrast-polarity edge cases), taking the pixelwise maximum across a discrete set of angles and selecting between the two candidates using a robust percentile-based separability score computed within the FOV.

The resulting enhancement map is converted into a per-pixel feature vector by pairing enhanced intensity with gradient magnitude (Sobel) to encode both tubular interior response and edge evidence, and k -means ($k = 2$) is fit deterministically (fixed RNG seed) on a capped random subset for efficiency. All FOV pixels are then assigned to the nearest centers, and the vessel cluster is selected as the one with higher mean enhancement response.

Finally, a compact post-processing stage (morphological closing/opening, connected-components filtering with an image-size-scaled minimum area threshold, and strict FOV

enforcement) removes speckle-like false positives and improves vessel continuity, yielding a reproducible binary (0/255) uint8 mask.

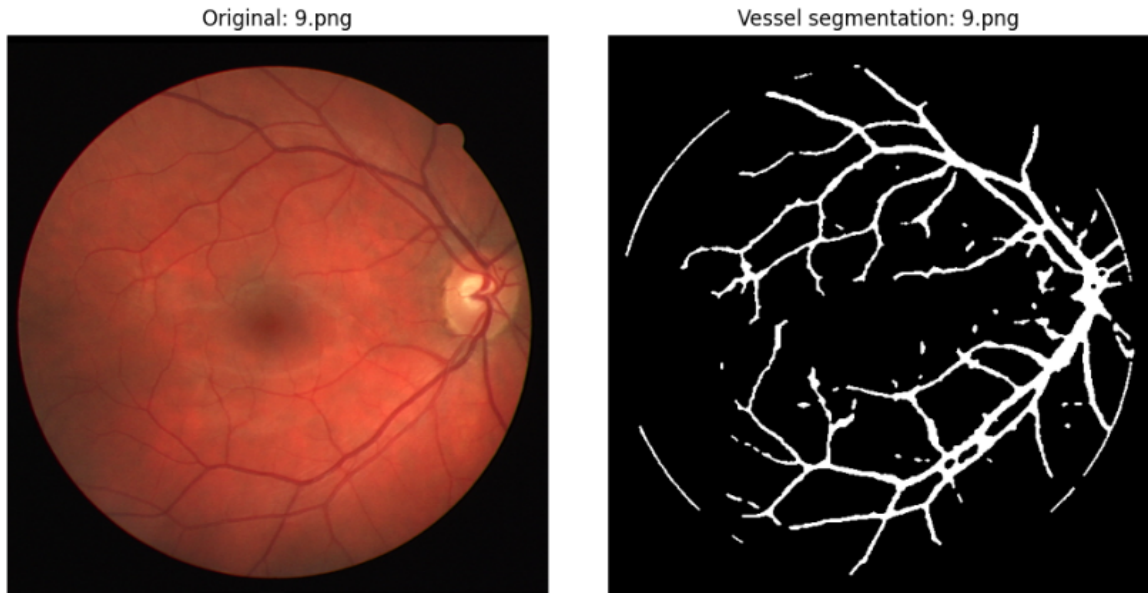


Figure 2.5: Vessel Segmentation for Image 8.png: IoU=0.554655

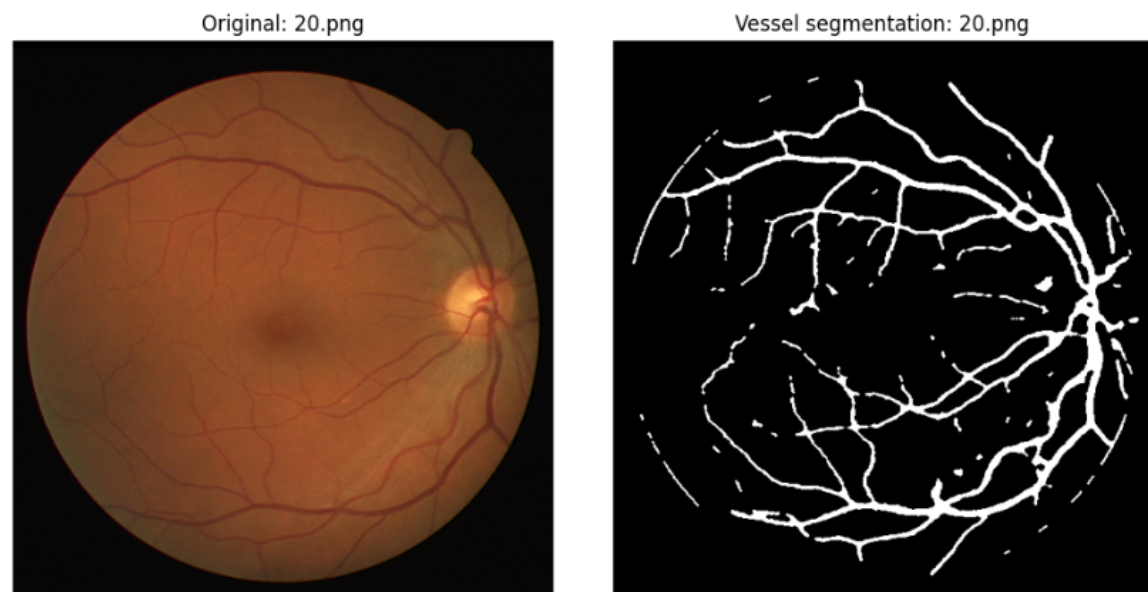


Figure 2.6: Vessel Segmentation for Image 13.png: IoU=0.549874

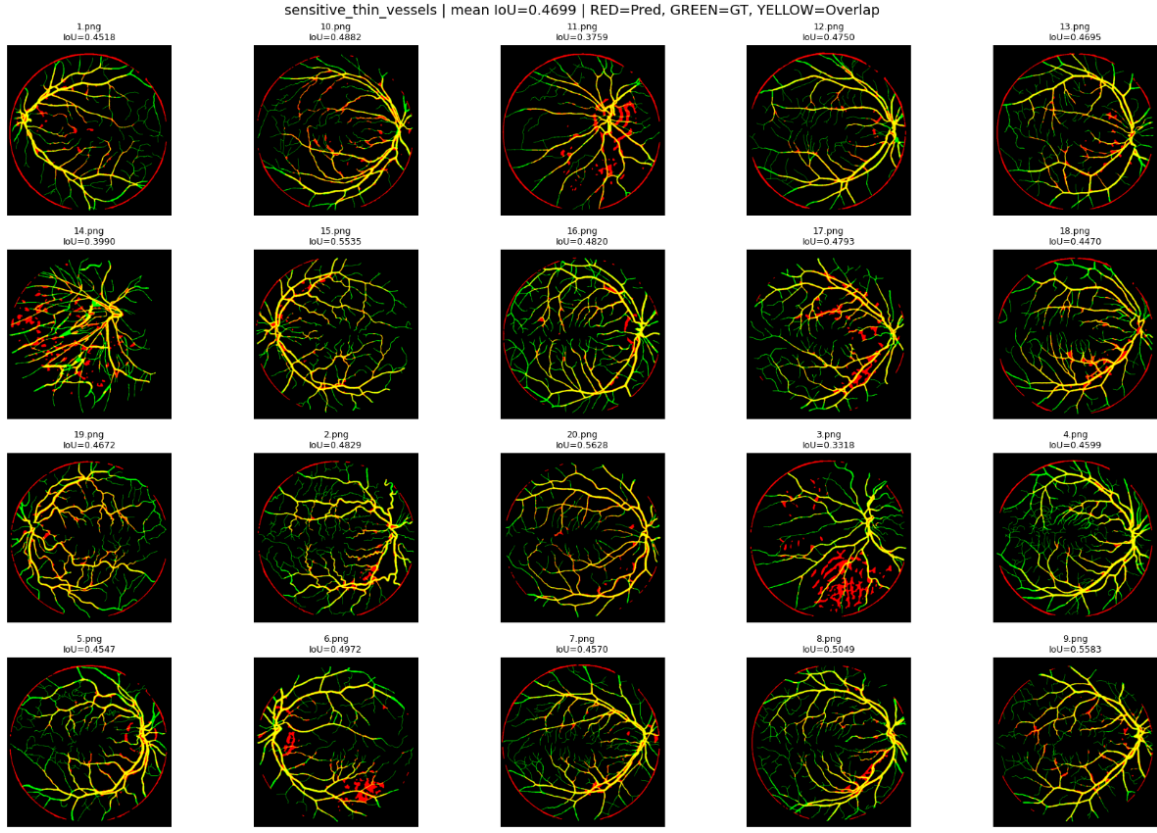


Figure 2.7: Best Grid for all Parameter Combinations for Pipeline B

Rank	Variant	Mean IoU	Median IoU	Std. IoU	Min IoU	Max IoU	Time (s/img)
01	fov_tight	0.516357	0.530119	0.059589	0.381341	0.590800	0.850982
02	balanced_plus_connect	0.501609	0.524085	0.064776	0.308627	0.570136	0.846812
03	clahe_strong_local	0.501579	0.512972	0.058309	0.326118	0.558490	0.887263
04	sensitive_thin	0.501285	0.520966	0.061377	0.322160	0.568212	1.061211
05	baseline_like_current	0.494634	0.506589	0.057131	0.374039	0.572505	0.954845
06	blackhat_forced	0.493499	0.503884	0.057712	0.365067	0.566992	0.825842
07	tophat_forced	0.493499	0.503884	0.057712	0.365067	0.566992	0.814135
08	no_grad_feature	0.484948	0.497850	0.061587	0.290911	0.561769	0.800040
09	k3_split_clusters	0.457601	0.456843	0.086860	0.319165	0.603578	1.017803
10	precision_fp_reduce	0.411471	0.419151	0.051825	0.311825	0.489197	0.833775

Notes. Performance summary for the evaluated variants in the retinal vessel segmentation task, sorted by mean IoU (higher is better). Runtimes are reported as seconds per image.

Table 2.2: Pipeline B variant ranking after grid search

2.3 Pipeline C: Illumination correction → vessel enhancement → Graph Cut

Illumination correction is implemented as a Retinex-like separation of reflectance from illumination by subtracting a large-scale Gaussian background estimate from the green channel (used for its superior vessel contrast), followed by min–max normalization and CLAHE to amplify local vessel–background separability under vignetting and optic-disc variability.

Vessel enhancement then produces a continuous *vesselness* map via multi-scale morphological black-hat filtering (elliptic structuring elements at several odd kernel sizes), taking the maximum response across scales, applying light Gaussian smoothing, and re-normalizing within the FOV for numerical stability.

Finally, graph-cut segmentation is realized through `cv.grabCut` in `GC_INIT_WITH_MASK` mode (i.e., a GMM-based graph-cut refinement): the unary seeds are derived directly from vesselness quantiles, with «sure background» assigned to low vesselness and outside-FOV pixels, and «probable/sure foreground» assigned to high vesselness pixels; minimum-seed safeguards are enforced to avoid empty-initialization failures, and a deterministic vesselness-threshold fallback is provided if GrabCut fails.

The resulting binary mask is then cleaned by morphological opening/closing and connected-components filtering to remove speckle noise and suppress tiny false positives, yielding a reproducible (0/255) `uint8` vessel segmentation that operationalizes the key insight of Zhao et al. (2015): graph cuts are most effective when driven by a well-constructed enhancement (unary) map and a robust initialization.

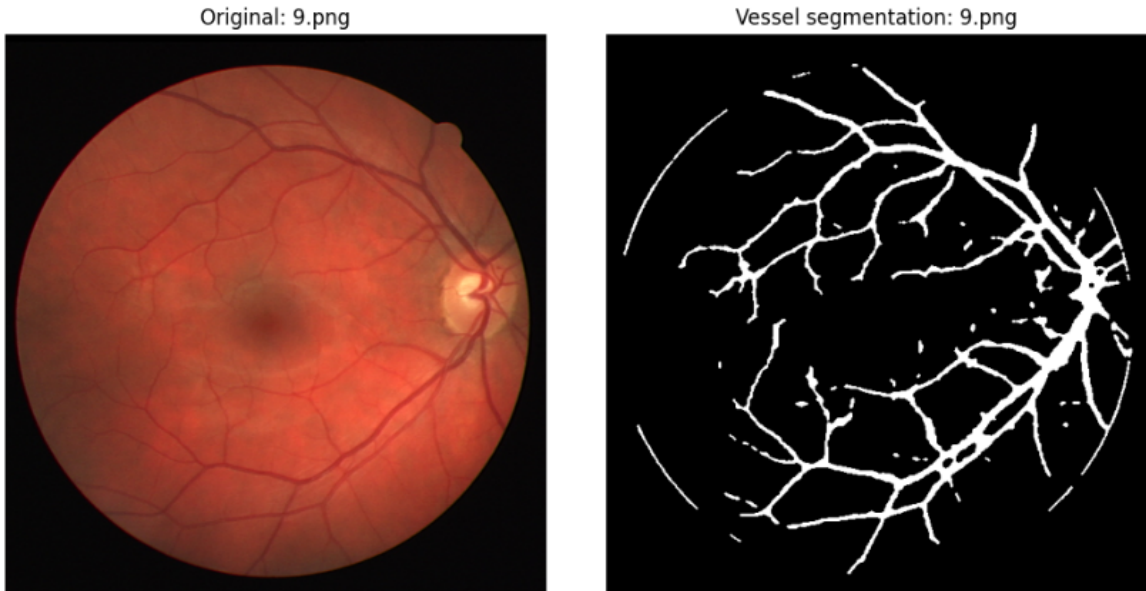


Figure 2.8: Vessel Segmentation for Image 9.png: IoU=0.558516

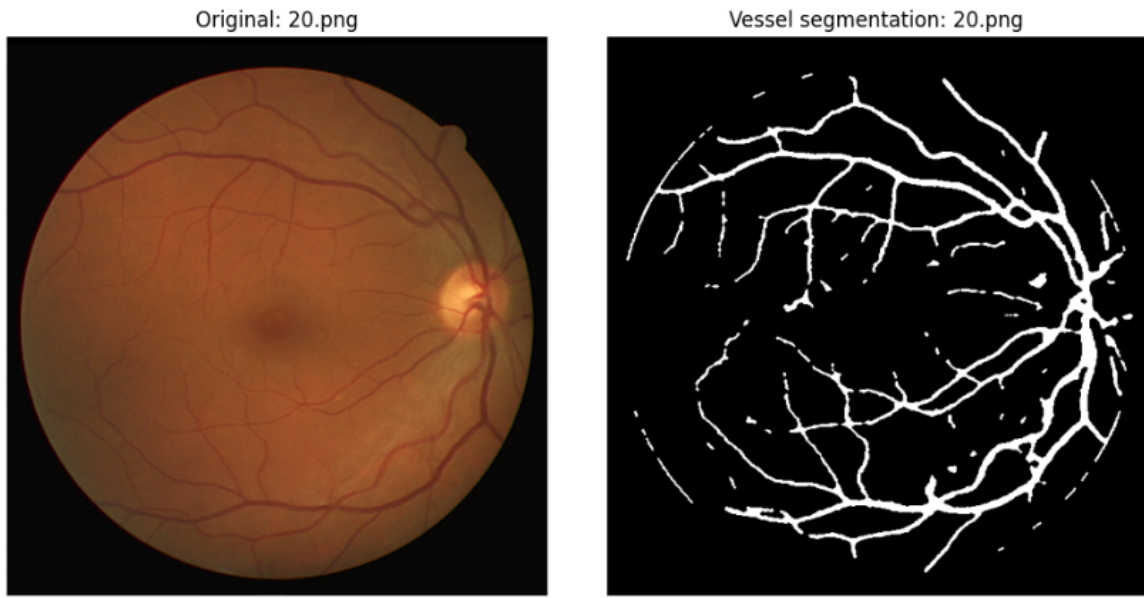


Figure 2.9: Vessel Segmentation for Image 20.png: IoU=0.562874

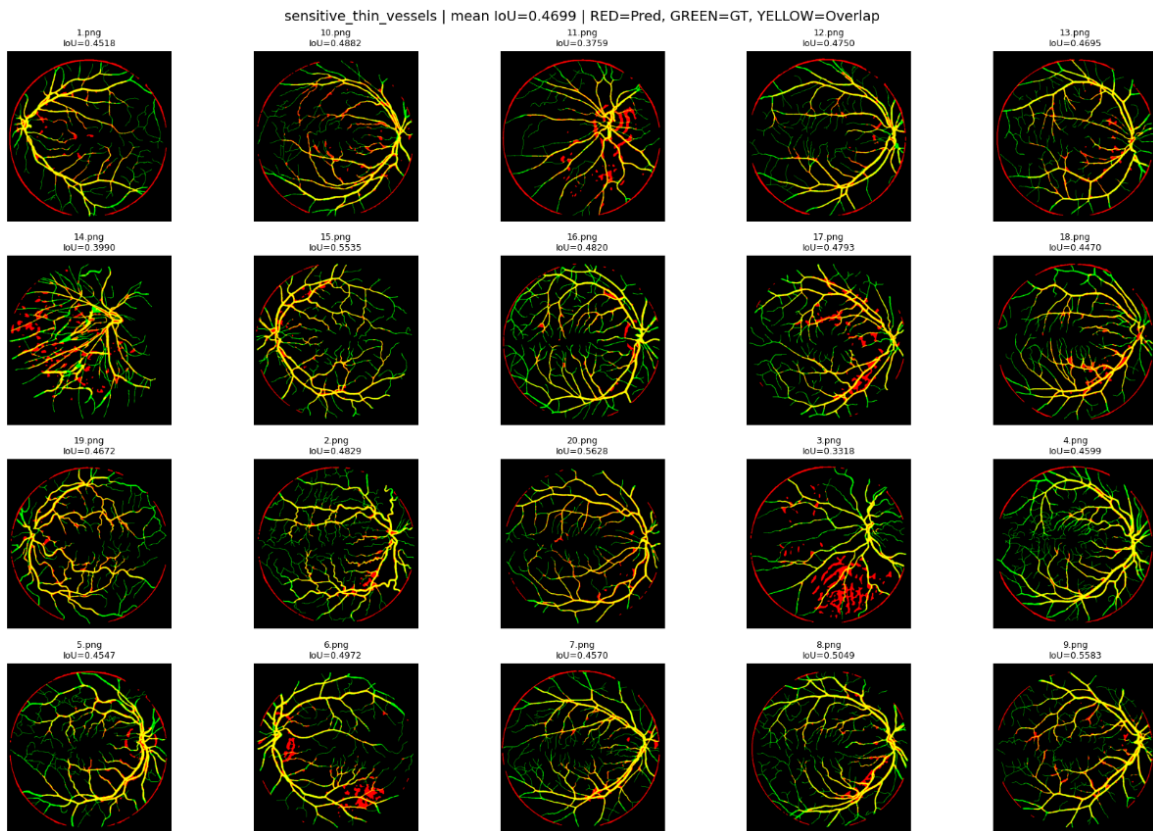


Figure 2.10: Best Grid for all Parameter Combinations for Pipeline C

Rank	Variant	Mean IoU	Median IoU	Std. IoU	Min IoU	Max IoU	Time (s/img)
01	sensitive_thin_vessels	0.469886	0.472241	0.054988	0.331782	0.562823	1.929633
02	minimal_smoothing_thin_edges	0.461301	0.462583	0.056539	0.314613	0.559406	1.810755
03	retinex_more_local_detail	0.409463	0.402876	0.051385	0.289363	0.499832	1.898789
04	strong_clahe_low_contrast_res	0.404641	0.404963	0.051979	0.276426	0.503435	2.090622
05	balanced_plus_connectivity	0.365085	0.361225	0.051571	0.268582	0.482957	2.222029
06	seed_heavy_grabcut_stability	0.356679	0.349522	0.054519	0.270706	0.481737	2.450296
07	baseline_defaults	0.345072	0.337279	0.054119	0.258204	0.472041	1.567069
08	precision_reduce_fp	0.216701	0.214032	0.044549	0.145411	0.319381	1.822385

Notes. Performance summary for pipeline variants (sorted by mean IoU; higher is better). Runtimes are reported as seconds per image.

Table 2.3: Pipeline C variant ranking after grid search

All of the different parameters used in each variant can be seen in the `.ipynb` file of the project.

2.4 Pipeline D: Multi-orientation morphology + connected

This Pipeline is an explicitly morphology-driven vessel segmentation pipeline in which mathematical morphology acts as the primary mechanism for both vessel enhancement and structural regularization, while connected-components analysis provides an interpretable, geometry-based rejection stage for non-vascular artifacts.

The implementation first restricts processing to anatomically valid pixels by computing a binary retinal field-of-view mask via `compute_fov_mask`, and then applies `segment_vessels_morphology` with a parameter object (`VesselMorphParams`) that exposes all key degrees of freedom.

Within the FOV, the green channel is optionally contrast-normalized with CLAHE (configured by `clahe_clip_limit` and `clahe_tile`) to increase local vessel–background separability, after which a multi-scale, multi-orientation line-enhancement stage is performed using line-shaped structuring elements sampled over several lengths and a dense set of angles (e.g., a uniform angular grid), computing a line-response map per orientation/scale and then aggregating them by a max operator to produce an orientation-invariant «morphological vesselness» response that preferentially amplifies elongated, dark tubular structures while suppressing slowly varying background.

The resulting response is binarized by an unsupervised thresholding rule (e.g., Otsu or a percentile-based threshold, depending on the election of the configuration) computed using only in-FOV pixels to avoid peripheral bias, and the preliminary mask is regularized with

small-kernel closing/opening (`post_close_ksize`, `post_open_ksize`) to reconnect short gaps and remove speckle.

Finally, connected components are filtered using simple motivated shape constraints—minimum area (`cc_min_area`), minimum elongation (`cc_min_elongation`), maximum extent (`cc_max_extent`) and a cap on relative component size (`cc_max_area_frac`)—so that compact blobs and large non-vessel regions are rejected while thin, elongated candidates are retained.

Conceptually, this design matches the «mathematical morphology» family emphasized in morphology-centric retinal pipelines (e.g., the morphology-based enhancement motivation in Hassan et al., 2015) and in broader reviews of classical vessel segmentation: the segmentation behavior is governed by physically interpretable parameters (structuring-element geometry, aggregation rule, and explicit shape filters).

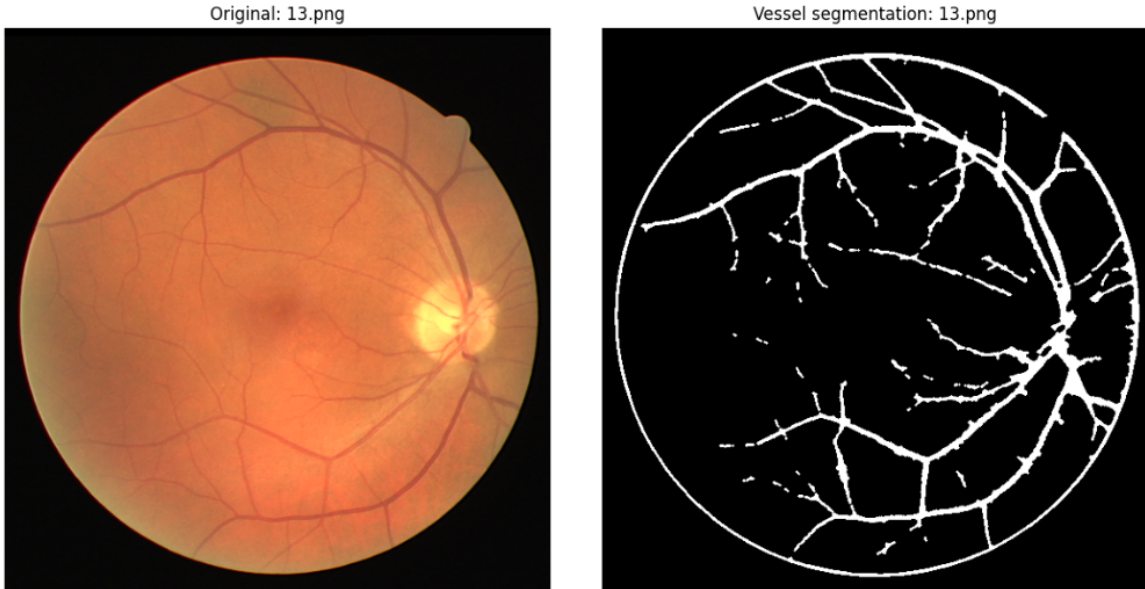


Figure 2.11: Vessel Segmentation for Image 13.png; IoU=0.455248

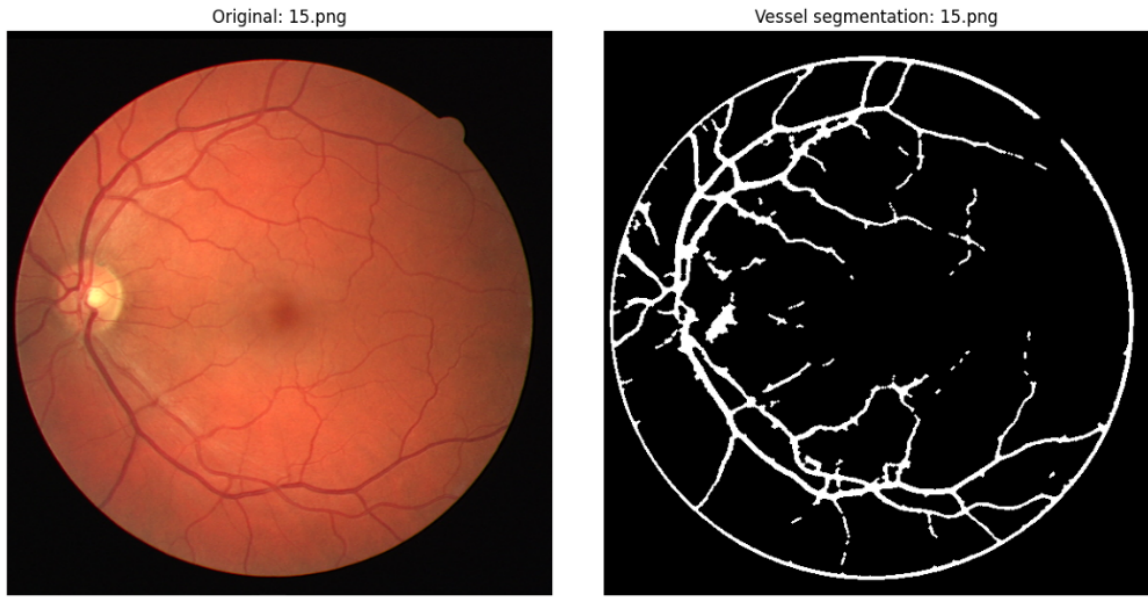


Figure 2.12: Vessel Segmentation for Image 15.png: IoU=0.431216

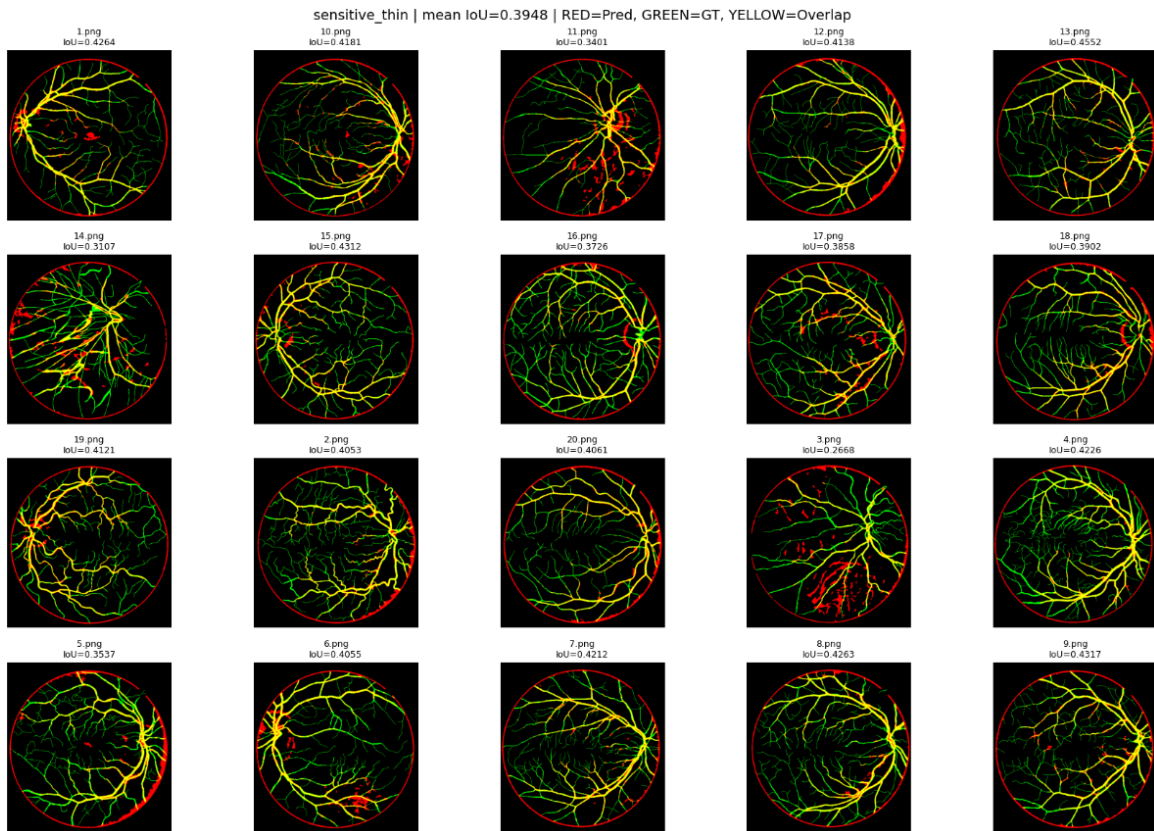


Figure 2.13: Best Grid for all Parameter Combinations for Pipeline D

Rank	Variant	Mean IoU	Median IoU	Std. IoU	Min IoU	Max IoU	Time (s/img)
01	sensitive_thin	0.394780	0.409087	0.044772	0.266801	0.455248	0.848891
02	reconnect_fragments	0.368714	0.380619	0.039489	0.261758	0.427330	0.843856
03	clahe_strong_boost	0.348571	0.356698	0.038419	0.249885	0.393831	0.831856
04	baseline_balanced	0.337998	0.345709	0.035341	0.260794	0.381608	0.792475
05	fov_tight_rim	0.291291	0.292910	0.046448	0.191943	0.371907	0.851015
06	fov_loose_recover	0.240899	0.246684	0.022095	0.189935	0.278500	0.846580
07	precision_fp_guard	0.170757	0.170155	0.033179	0.104169	0.231828	0.807830
08	noise_harsh_cleanup	0.085827	0.090114	0.033987	0.007811	0.145737	0.799394

Notes. Performance summary for the evaluated pipeline variants (sorted by mean IoU; higher is better). Runtimes are reported as seconds per image.

Table 2.4: Pipeline D variant ranking after grid search

All of the different parameters used in each variant can be seen in the `.ipynb` file of the project.

2.5 Pipeline E: Use of CC mainly as structural filtering, not as a primary segmenter

This Pipeline implements a **connected-components–driven structural filtering stage** that is deliberately positioned *after* a conventional, unsupervised «vessel candidate» generator, thereby treating connected components not as a primary segmenter but as a mechanism to **enforce vascular geometry and reject anatomically implausible detections**.

After computing the FOV mask and extracting the grayscale channel, It then performs a Retinex-inspired inhomogeneity correction (`_retinex_bilateral`) by taking a log-domain difference between the image and an edge-preserving bilateral-smoothed illumination estimate.

Local contrast is further strengthened via CLAHE (`_clahe`), and a vesselness-like response is produced using **multi-scale, multi-orientation morphological black-hat filtering** with explicitly constructed line structuring elements (`_multiscale_multiorient_blackhat` with `_line_kernel`), which encodes the prior that vessels are **dark, elongated structures across multiple orientations**.

The resulting response is normalized within the FOV and binarized using an Otsu threshold computed only over masked pixels (`_masked_otsu_threshold`), optionally shifted by `thr_offset` to control sensitivity. A lightweight opening/closing post-step reduces speckle and reconnects micro-gaps without substantially thickening vessels.

The **core contribution** then applies `connectedComponentsWithStats` and removes

components using interpretable shape constraints computed per component (`_component_shape_metrics`): minimum area (hard and conditional on elongation), **circularity** (to reject round/compact blobs), **extent** (to penalize filled bounding boxes typical of lesions/artifacts), and **elongation** estimated via PCA eigenvalue ratios over foreground coordinates, retaining only components that are sufficiently elongated and non-blob-like.

This design operationalizes the key principle that connected components «do not create vessels», but rather **filter candidate pixels into a topology that better matches a vessel tree**, and it is instrumented with optional verbose diagnostics (foreground fractions, percentiles, threshold values, and removal statistics)

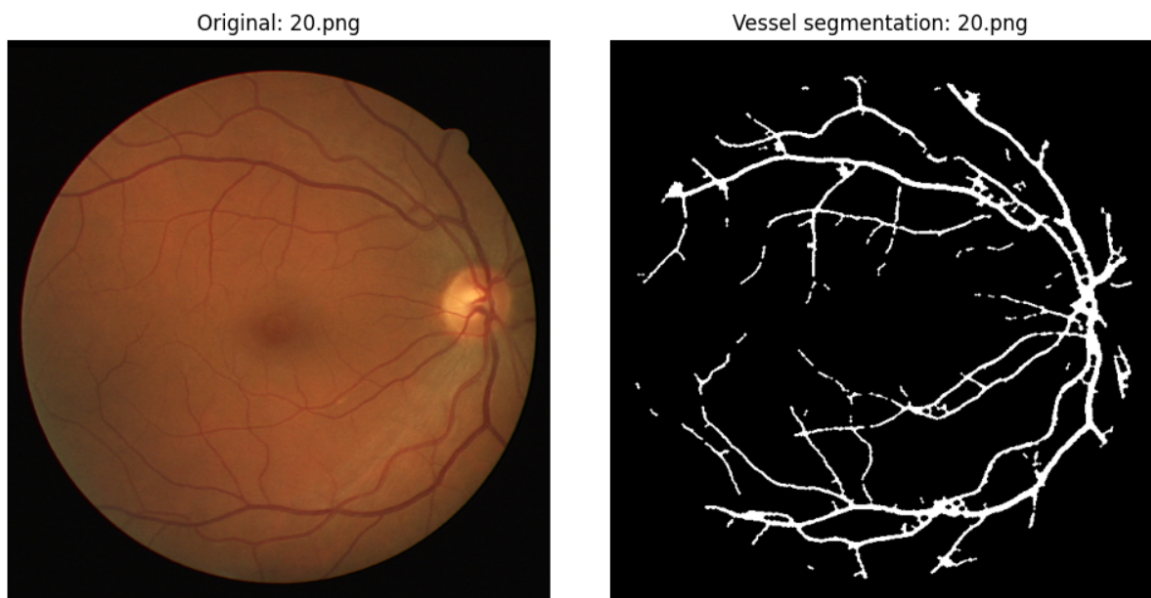


Figure 2.14: Vessel Segmentation for Image 20.png: IoU=0.560231

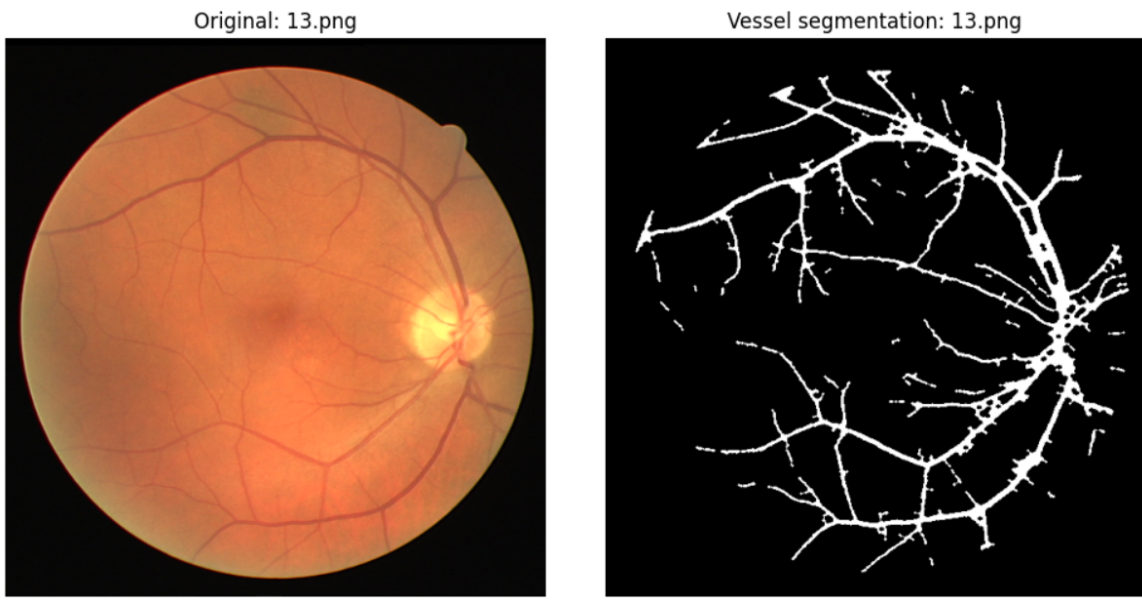


Figure 2.15: Vessel Segmentation for Image 13.png: IoU=0.556936

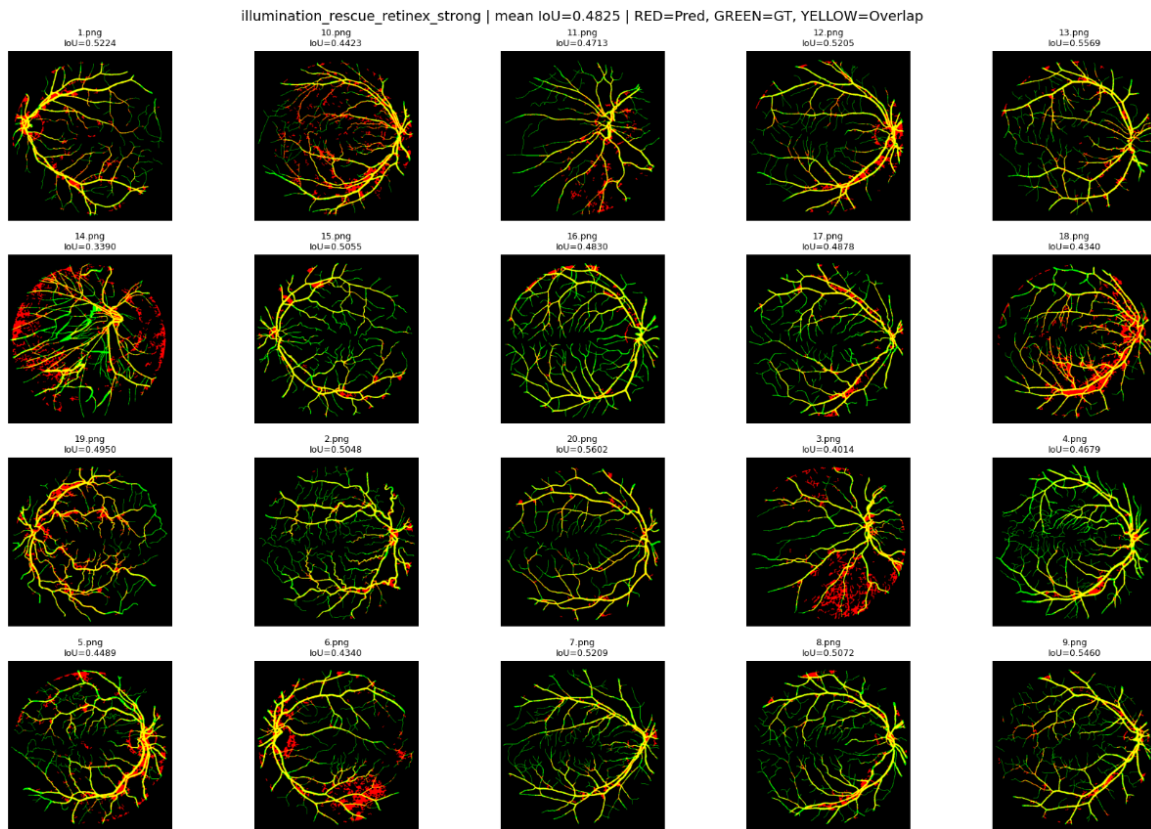


Figure 2.16: Best Grid for all Parameter Combinations for Pipeline E

Rank	Variant	Mean IoU	Median IoU	Std. IoU	Min IoU	Max IoU	Time (s/img)	Pred. FG frac.
01	illumination_rescue_retinex_strong	0.482461	0.491398	0.053344	0.338991	0.560231	1.523021	0.083416
02	smooth_vesselness_reduce_speckle	0.477865	0.518488	0.085937	0.254895	0.569876	2.728567	0.098809
03	baseline_default	0.455043	0.467818	0.049298	0.324895	0.537293	2.311612	0.056290
04	sensitivity_thin_vessels	0.415537	0.458196	0.079089	0.271901	0.500810	1.930595	0.126949
05	dense_orientations_thin_focus	0.413728	0.451665	0.086221	0.261653	0.508157	1.896875	0.129335
06	blob_suppress_aggressive_cc	0.398045	0.398085	0.086095	0.250773	0.502657	1.762109	0.139274
07	balanced_plus_reconnect	0.377030	0.380178	0.088892	0.228346	0.488676	1.565580	0.154732
08	precision_fp_reduction	0.140230	0.136051	0.047157	0.047360	0.241871	0.980021	0.012826

Notes. Performance summary for the evaluated variants (sorted by mean IoU; higher is better). Runtimes are reported as seconds per image. *Pred. FG frac.* denotes the mean fraction of pixels predicted as foreground (useful to diagnose over/under-segmentation).

Table 2.5: Pipeline E variant ranking after grid search

All of the different parameters used in each variant can be seen in the *.ipynb* file of the project.

3. Comparison and Conclusion

The following table compares all the versions of the Pipelines and the obtained results discussed before:

Rank	Pipeline	Variant	Mean IoU	Median IoU	Std. IoU	Min IoU	Max IoU	Time (s/img)
01	A	strong_clahe	0.552167	0.576725	0.069193	0.334794	0.614325	0.692420
02	B	fov_tight	0.516357	0.530119	0.059589	0.381341	0.590800	0.850982
03	E	illumination_ rescue_retinex_ strong	0.482461	0.491398	0.053344	0.338991	0.560231	1.523021
04	C	sensitive_thin_vessel	0.469886	0.472241	0.054988	0.331782	0.562823	1.929633
05	D	sensitive_thin	0.394780	0.409087	0.044772	0.266801	0.455248	0.848891

Table 3.1: Best variant per pipeline after grid search (IoU statistics, runtime, and foreground fraction when available)

Across the best-performing variants of each pipeline, Pipeline A (`strong_clahe`) emerges as the most accurate approach, achieving the highest mean IoU (0.552167) and median IoU (0.576725), with a competitive runtime (0.692420 s/img), indicating that a carefully tuned sequence of green-channel contrast enhancement (CLAHE) plus morphology-driven vessel boosting and unsupervised thresholding provides the strongest overall separability between vessels and background in this dataset.

Pipeline B (`fov_tight`) ranks second (mean IoU 0.516357; median 0.530119) and is comparatively stable, as reflected by its relatively low dispersion (std 0.059589) and notably high minimum IoU (0.381341), suggesting fewer catastrophic failures even if the average accuracy remains below Pipeline A. This robustness is obtained at a modest runtime penalty (0.850982 s/img), likely due to the additional clustering stage.

Pipelines E and C, despite incorporating more sophisticated illumination handling (Retinex-like correction) and downstream structural refinement (connected-components filtering in E; graph-cut refinement in C), do not translate this added complexity into superior IoU: their mean IoUs remain lower (0.482461 and 0.469886, respectively) while runtimes increase substantially (1.523021 and 1.929633 s/img), indicating that, under the present parameterization and data regime, these mechanisms improve neither the central tendency nor the speed–accuracy trade-off.

Finally, Pipeline D (`sensitive_thin`) exhibits the weakest segmentation quality (mean

IoU 0.394780; max 0.455248), showing that morphology and component filtering alone, without stronger contrast/illumination normalization and threshold stabilization, is insufficient for reliable vessel delineation.

To conclude, we can state that the experimental evidence supports Pipeline A as the most effective and practical solution—delivering the best accuracy with a favorable runtime—while Pipeline B constitutes a reasonable alternative when prioritizing stability against worst-case images. Conversely, the higher-cost refinements in Pipelines C and E would require further methodological or parameter redesign to justify their computational overhead.

Finally, regarding the main issues encountered, the most challenging aspect for me was debugging cases where certain images achieved a good IoU while others performed poorly. Addressing this required carefully handling image-specific characteristics, such as darker regions in the green channel or reduced vessel visibility due to lower effective resolution in some samples.

In addition, identifying the best hyperparameter combinations proved difficult, since it is not straightforward and it is impossible to know in advance which setting will yield the strongest performance. To tackle this effectively, adopting a grid-search methodology was particularly valuable.